Peptide-functionalized Gold Nanoparticles: Versatile Biomaterials for Diagnostic and Therapeutic Applications

Jingyi Zong,[a] Steven L. Cobb[a] and Neil R. Cameron[b,c,*]

[a] Department of Chemistry, Durham University, South Road, Durham, DH1 3LE, U.K.

[b] Department of Materials Science and Engineering, Monash University, Clayton, 3800, Victoria, Australia

[c] School of Engineering, University of Warwick, Coventry, CV4 7AL, U.K.

*****Email address: neil.cameron@monash.edu

Abstract

Colloidal gold solutions have been used for centuries in a wide variety of applications including staining glass and in the colouring of ceramics. More recently, gold nanoparticles (GNPs) have been studied extensively due to their interesting size-dependent electronic and optical properties. GNPs can be functionalized easily with biomolecules that contain thiols, amines, or even phosphine moieties. For example, the reaction of thiol-containing peptides with GNPs has been used extensively to prepare novel hybrid materials for biomedical applications. A range of different types of peptides can be used to access biomaterials that are designed to perform a specific role such as cancer cell targeting. In addition, specific peptide sequences that are responsive to external stimuli (e.g. temperature or pH) can be used to stabilise / destabilise the aggregation of colloidal GNPs. Such systems have exciting potential applications in the field of colorimetric sensing (including bio-sensing) and in targeted drug delivery platforms. In this review, we will give an overview of the current methods used for preparing peptide functionalized GNPs, and we will discuss their key properties outlining the

various applications of this class of biomaterial. In particular, the potential applications of peptide functionalized GNPs in areas of sensing and targeted drug delivery will be discussed.

1. Introduction

Colloidal gold solutions have been known and used, since ancient times, for staining glass and colouring ceramics. In more recent times, gold nanoparticles (GNPs) have been extensively studied due to their size dependent electronic and optical properties.[1, 2] In the early 1950s, Turkevich developed an approach for the synthesis of GNPs[3], which involved the reduction of hydrogen tetrachloroaurate (III) ($HAuCl_4$) in water by a reducing agent/stabilising ligand, such as sodium citrate. Using this process, GNPs with a size ca. 20nm can be prepared. Later, Frens improved this method and obtained GNPs with a more controlled diameter (between 16 and 147 nm).[4] In this later approach, the trisodium citrate to gold ratio controls the size of the GNPs: a higher ratio gives a smaller particle size. GNPs can be easily functionalized with biomolecules which contain thiols, amines, or even phosphine moieties. The most common approach is to functionalize GNPs with thiol containing molecules. Using this method it has been possible to synthesize novel hybrid materials consisting of combinations of GNPs and proteins (or peptides). The peptides and proteins utilised in these systems can fulfil different roles, acting as drug carriers, anti-cancer drugs and even cellular targeting moieties.[5, 6]

In the last decade, a variety of peptide functionalized GNPs have been synthesized and applied in a range of areas including bio-detection, targeted drug delivery and cellular uptake studies.[7-10] Adding peptides to citrate-capped GNPs can produce highly stable peptide-capped nanoparticles even in an aqueous buffer. The ability to assemble/disassemble GNPs can be modulated by changing the peptide sequence. For example, pH-responsive peptides can alter

their conformation in response to changes in their local environment and this can lead to aggregation of GNPs which will itself give rise to a visual colour change.[11]

In this review, the discussion will focus primarily on the different methods of preparing peptide functionalized GNPs, their properties and their use in various biomaterials applications. In particular, applications in the areas of metal ion and molecular detection and targeting drug delivery will be discussed in more detail.

2. Synthesis of Peptide-functionalized Gold Nanoparticles (GNPs)

Generally, a colloidal gold solution is produced by the reduction of chloroauric acid ($HAuCl_4$). The Frens method is the simplest approach to produce citrate-capped nanoparticles of controlled diameter[4]. The resulting citrate-GNPs have been further functionalized with different peptides to improve their stability. There are three main approaches of preparing peptide-functionalized GNPs: (1) ligand exchange; (2) chemical reduction; and (3) chemical conjugation.

2.1 Ligand Exchange

The ligand exchange method is the most commonly used approach to prepare peptide-GNPs. It essentially involves displacement of one ligand for another,[12, 13] and was first explored by Hostetler *et al.*[12] who attempted to replace simple thiol ligands on GNPs with more complex thiols. The ligand exchange method has been used successfully to synthesise a range of GNPs capped with cysteine-containing peptides. Tetrachloroaurate ions ($AuCl_4^-$) are firstly reduced by sodium citrate and citric acid to give citrate-stabilized GNPs. In the presence of Cys-capped peptides the citrate-stabilized GNPs undergo ligand exchange to give peptide

functionalized GNPs.[14, 15] This reaction proceeds as the cysteine containing peptides have a stronger interaction with the GNPs compared to the citrate ions. The sulfur-gold bond has a strength of approximately 210 kJ mol^{-1}.[16] This ligand exchange method is very useful when the desired thiol ligand is valuable or not compatible with the reductive environment. A single thiol group can already be quite strong as a binding ligand to a gold surface, however, in some complex systems, multiple thiols may be desired if higher chemical stability is required. For example, Lin *et al.*[17] reported a two-step method to attach neutral and positively charged thiols onto the gold surface (Figure 1). The first step is to reduce tetrachloroauric acid with sodium citrate and then replace the citrate with thioctic acid (TA). In the second step, TA is replaced by functional groups containing thiols. Through the two-step approach, stable gold nanoparticles can be functionalized with a wide range of thiols including those bearing positive charges.

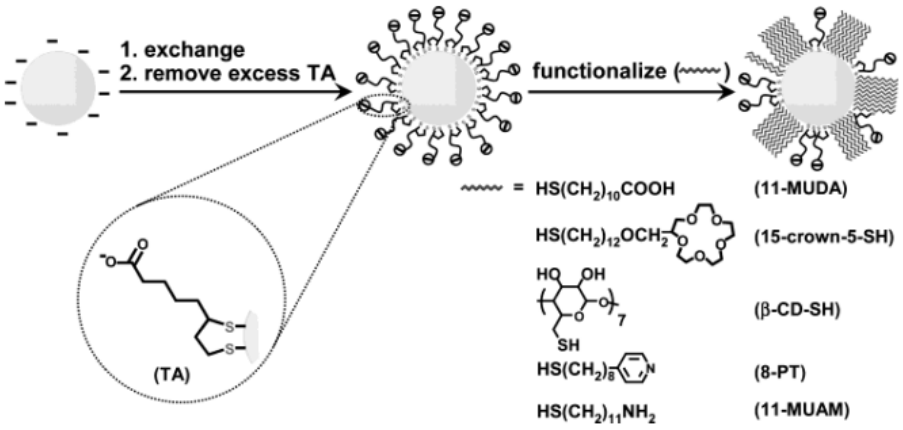

Figure 1. A two-step modification method for functionalising gold nanoparticles.[17] Reprinted with permission from S.-Y. Lin, Y.-T. Tsai, C.-C. Chen, C.-M. Lin and C.-H. Chen, J. Phys. Chem. B, 2004, 108, 2134-2139. Copyright 2004 American Chemical Society.

2.2 Chemical Reduction

In 2005, Bhattacharjee *et al.*[18] reported an approach to prepare colloidal GNP-tripeptides through an *in situ* tyrosine reduction technique. The designed tripeptide sequence was H_2N-Leu-Aib-Tyr-OMe (Aib is 2-aminoisobutyric acid, or 2-methylalanine); tyrosine was included at the C-terminus to act as an electron-transfer agent.[19] The tyrosine reduces $AuCl_4^-$ to Au^0, and the free amine at the N-terminus of the tripeptide can attach to the gold surface resulting in a colloidal suspension. The size of the tripeptide-GNPs prepared via this approach was relatively small, around 8.7 nm. However, when excess tri-peptides were added to a gold salt solution, the resultant tripeptide-GNPs aggregated due to H-bonding between the terminal NH_2 group and side chains of amino acid residues. Other tyrosine containing peptides have also been used to synthesise peptide-GNPs. For example, the peptide NPSSLFRYLPSD was used to reduce gold ions to GNPs and subsequently form organic-inorganic hybrid nanoparticles.[20] Higher temperatures decreased the size of the nanoparticles that were obtained.

In 2009 Serizawa *et al.*[21] reported another method for the synthesis of peptide functionalised GNPs by reduction using HEPES buffer. The reduction was carried out in the presence of Cys-terminal basic peptides under ambient conditions. This approach solved the difficulties typically associated with the functionalization of GNPs with peptides containing basic amino acids, such as Arg-Pro-Thr-Arg (RPTR), which tends to result in GNP aggregation and precipitation.

2.3 Chemical Conjugation

Generally, GNPs are formed in aqueous solution and capped by water-soluble stabilizers, such as thiolated derivatives of PEG, glutathione or mercaptosuccinic acid. These stabilizers

often have active sites that can be used to bind peptides and other biomolecules. This method of combining peptides to GNPs is known as the chemical conjugation method.

In 2009, Xie *et al.*[22] showed that nuclear localization signal (NLS) peptide functionalized-GNPs can be used as a nuclear targeting nanoprobe. The nanoparticles were first modified by 11-mercaptoundecanoic acid (11-MUA), and the NLS peptide was then connected to the modified GNPs by carbodiimide coupling (Figure 2). Bartczak and co-workers[23] developed a one-pot synthesis method using EDC/sulfo-NHS (N-hydroxy sulfosuccinimide) coupling to conjugate the peptide KPQPRPLS to carboxy-terminated oligoethyleneglycol gold nanoparticles (OEG NPs). The degree of peptide coupling was affected by experimental parameters, such as reaction time, concentration of reagent and the morphology of the nanocrystal.

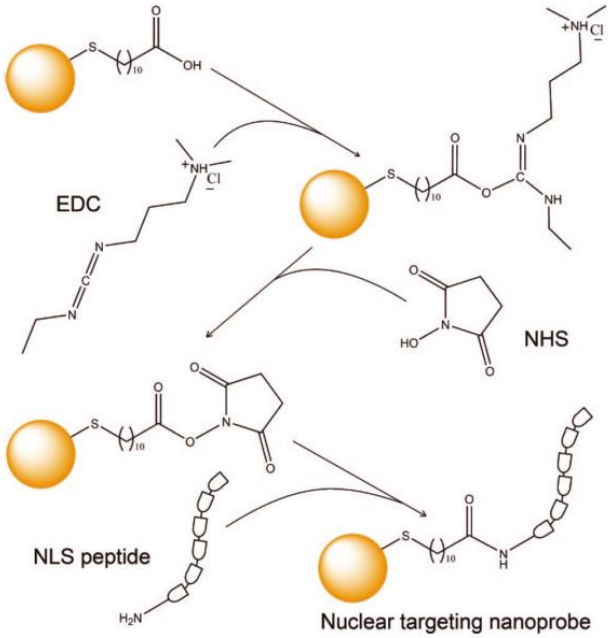

Figure 2. Preparation of nuclear localising signal peptide-functionalised gold nanoparticles.[22] Reprinted with permission from W. Xie, L. Wang, Y. Zhang, L. Su, A. Shen, J. Tan and J. Hu, Bioconjug. Chem., 2009, 20, 768-773. Copyright 2009 American Chemical Society.

3. Properties of Peptide-Functionalized Gold Nanoparticles

3.1 pH Responsiveness

The first detailed study of reversible self-assembly of peptide-capped GNPs at different pH values was reported by Mandal *et al*. in 2007.[11] The tyrosine reduction technique[18] was used to obtain GNPs functionalised with H_2N-Leu-Aib-Tyr-OMe. UV-vis spectroscopy showed that when the pH decreased, the surface plasmon resonance (SPR) band displayed a red shift along with a visual colour change of the peptide-GNP from red to violet. This indicates GNP assembly due to H-bonding between –COOH groups on the gold surface when the solution pH is near the pKa of the carboxylic acid. TEM results showed that the peptide-GNPs formed a network of 1D chains at pH 4; when the pH decreased below 4, assemblies of 2D nanostructures and, finally, 3D structures, were observed as shown in Figure 3. When the pH was increased to 7, the peptide-GNPs disassembled again, demonstrating reversibility. The process is driven only by peptide H-bonding interactions, as evidenced by the fact that when the same UV-vis experiments were carried out using un-functionalized GNPs, no assembly occurred. This work demonstrates that carboxylated peptide-functionalized GNPs can be affected by pH to give assembly/disassembly driven by H-bonding interactions.

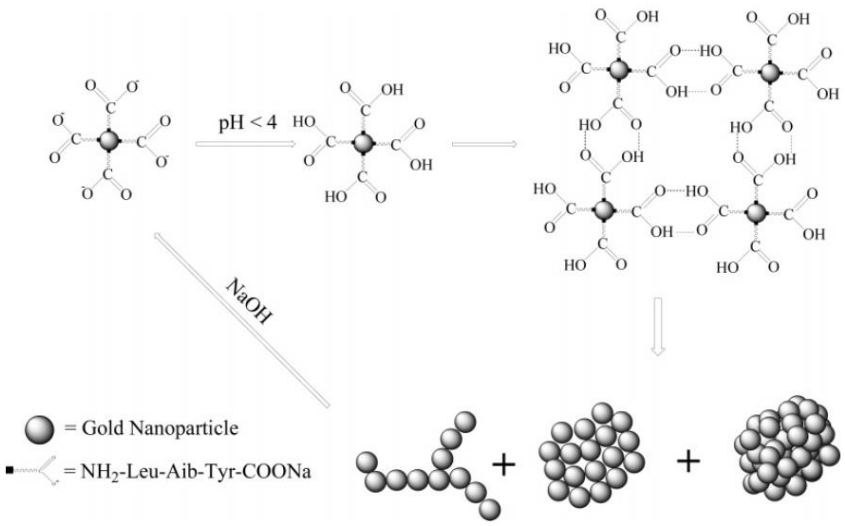

Figure 3. Self-assembly and disassembly of pH-responsive peptide-GNPs.[11] Reprinted with permission from S. Si and T. K. Mandal, Langmuir, 2007, 23, 190-195. Copyright 2007 American Chemical Society.

In 2010, van Hest *et al.*[24] reported the preparation of elastin-like peptide (ELP) functionalised GNPs, which are temperature and pH responsive. In their system, the short ELP VPGVG was used to functionalise GNPs through a ligand-exchange reaction. VPGVG undergoes a structural transition from a hydrophilic random coil to a hydrophobic β-spiral when the temperature is increased. The same behaviour was expected of the VPGVG-GNPs, however the VPGVG-GNPs solutions showed no LCST until the pH value dropped below pH 3.3. UV-visible spectroscopy demonstrated that the transition temperature is pH dependent, and the LCST varies from 14 to 41°C when the pH changes from 2.1 to 3.3. This is due to the fact that the VPGVG peptide has a free carboxylic acid at the C-terminus, which is protonated at low pH leading to a more hydrophobic VPGVG peptide. The VPGVG-GNPs displays the same LCST behaviour, which can be modulated by altering pH.

Minelli *et al.*[25] designed stimuli responsive 1.4 nm GNPs functionalised with a pH sensitive coiled coil peptide (pHcc) to obtain a reversible system sensitive to environmental pH. The peptide sequence was Ac-CGGGE-Helix-$CONH_2$, where the helix sequences is VSALENE-VAKLKNE-VKYLEAE-VARLKNE-VEFLEK. The pHcc peptide undergoes a reversible conformational change from a α-helix to random coil when the pH is increased from 2 to 7. Due to this behaviour, the pHcc can bind to a GNP surface via coiled coil assembly at pH 4, however at pH 7 the binding does not occur because the conformation changes to a random coil. This strategy can be applied to reversible molecular binding by pH control.

3.2 Enhanced stability for use in biological environments

In 2004 Levy *et al.*[14] developed Cys-Ala-Leu-Asn-Asn (CALNN) stabilized GNPs. This peptide gives extremely stable, water-soluble GNPs which can be further functionalized with biomolecules. The cysteine (C) at the N-terminus is able to form a linkage to the gold surface, while the interior hydrophobic amino acids alanine (A) and leucine (L) promote peptide self-assembly. The hydrophilic asparagine (N) which has a negative charge at the C-terminus is exposed to the external aqueous solution. This designed pentapeptide-functionalized GNP is stable at different pH values and in various buffer ionic strengths. More importantly, CALNN-GNPs remain stable even when decorated with longer peptides or proteins which opens up options to develop biological applications for this system. Subsequently, Wang *et al.*[26] prepared CALNN-GNPs functionalised with both DNA and biotin in a single easy step preparation. These particles exhibit specific binding ability to DNA and protein microarrays via their biological functionalities. This approach could be applied to a variety of peptide recognition motifs with high specificity and affinity.

Krpetic and coworkers [15] designed a peptide with four cysteine moieties to produce GNPs of enhanced stability. The peptide, named GCK15, has the sequence GCGGCGGKGGCGGCG; TEM, UV-Vis and FT-IR data showed that uniform GCK15-GNPs formed with no aggregation. In this system, the GCK15 'multi-dentate' peptide not only provides stable gold nanoparticles, but also has a single lysine residue which can be further functionalized.

'Stealth' peptide-capped GNPs which do not aggregate even in high salt solutions or in human serum were reported in 2014 by Nowinski *et al.*[27] The repeated glutamic acid (E) and lysine (K) amino acids in the peptide EKEKEK create a hydration layer that resists protein adsorption. Viability assays with endothelial cells and macrophages showed that EKEKEK-GNPs are not toxic in all test concentrations and resist internalisation. However, when a cyclic RGD was combined with the EKEKEK peptide, the cRGD-EK-GNPs were taken up efficiently. Therefore, the peptide-coated GNPs provide a very stable and stealthy nanoparticle system, which could possibly achieve long blood circulation half-life. Also, their stealth property can be altered by adding specific cell uptake motifs.

3.3 Self-assembly

Increasingly, studies are focusing on designed self-assembling structures and hybrid nanomaterials, aiming at building synthetic polypeptides with the same chemical flexibility as proteins but which have sensitivity to environmental changes and which can reversibly change their conformation. There are two methods commonly used to control peptide-GNP self-assembly: protease action or metal-ion complexation.

In 2007, Laromaine *et al.*[28] reported a short peptide-functionalized GNP system in which the assembly was controlled by the protease thermolysin, which catalyses the hydrolysis of

peptides containing hydrophobic amino acids. The tri-peptide sequence Fmoc-Gly-Phe-Cys-NH_2 was attached to the gold surface, and underwent self-assembly because of the Fmoc groups' π-stacking ability. When thermolysin was added into the solution, the amide bond between Gly and Phe was hydrolysed and disassembly occurred immediately, producing a clear colour change (Figure 4). This simple and very sensitive method offered a means by which to develop colorimetric assays to detect the presence of proteases.

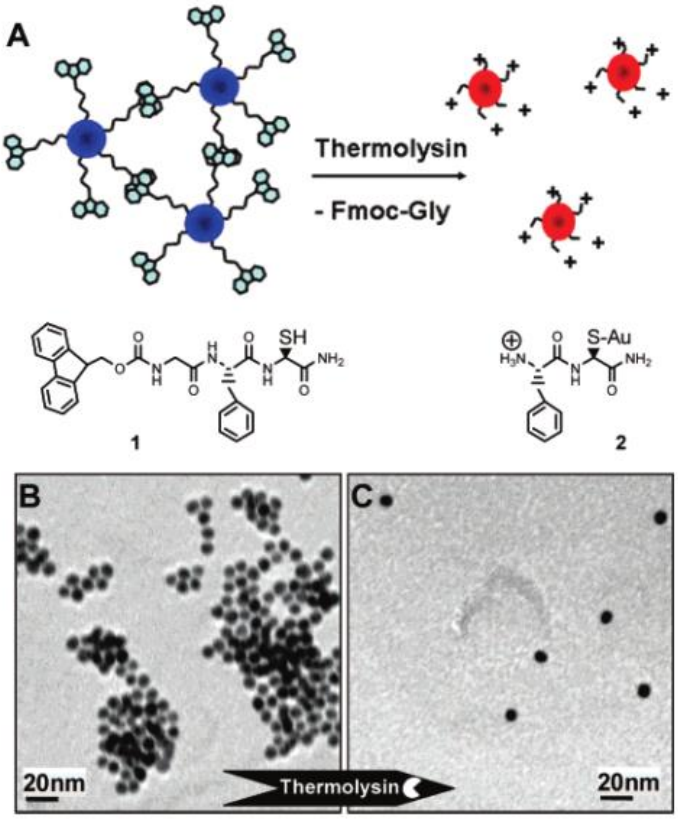

Figure 4. (A) GNP dispersion upon inclubation with a protease; (B) TEM image showing GNPs functionalized with Fmoc-Gly-Phe-Cys-NH_2; (C) TEM image of system in (B) following addition of thermolysin.[28] Reprinted with permission from A. Laromaine, L. Koh, M. Murugesan, R. V. Ulijn and M. M. Stevens, J. Am. Chem. Soc., 2007, 129, 4156-4157. Copyright 2007 American Chemical Society.

Aili *et al.*[29] studied the reversible assembly of polypeptide-coated GNPs by adding a polypeptide linker which can associate with immobilized surface peptides in a folding-dependent manner. JR2EC, a glutamic acid-rich, 42 residue peptide (NAADLEKAIEALEKHLEAKGPCDAAQLEKQLEQAFEAFERAG), was used to functionalise gold nanoparticles. It has a random coil structure at pH 7 but can change into a four-helix bundle structure when the pH is lower than 6, or in the presence of Zn^{2+}.[30] The JR2EC-functionalized GNPs dispersed in EDTA containing buffer were stable, while aggregation was observed when polypeptide $JR2KC_2$ (NAADLKKAIKALKKHLKAKGPCDAAQLKKQLKQAFKAFKRAG) was added. The $JR2KC_2$ peptide associates with helix-loop-helix peptide JR2EC and folds into two disulphide-linked four-helix bundles. The disulphide bridge can be removed by adding tris(2-carboxyethyl)phosphine (TCEP), resulting in slow redispersion of the aggregated GNPs. In this study, the optical property of GNPs was an important tool to demonstrate the molecular interaction.

Subsequently, a novel method of colorimetric protein assay based on the concept of reversible assembly of polypeptide-coated GNPs was developed.[31] The recognition is designed using a peptide sensor which can bind to the enzyme human carbonic anhydrase *II* (HCA*II*). In the absence of HCA*II,* the GNPs aggregate strongly which gives a large red shift of the plasmon peak. When there is HCA*II,* the immobilized peptides on the gold surface bind to the enzyme and prevent the GNPs from aggregating, leading to no colour change. This is because the steric hindrance by the bound enzyme prevents the folding of the immobilized polypeptides. The clear colour shift provides a very simple sensor which can be detected by the naked eye. They also proved that this detection system can be used to recognize a peptide sequence (C-pTMVP) form an antibody fragment (Fab57P). The

polypeptide-coated gold nanoparticles are very stable over a long time period and hence they have the potential to be applied in colourimetric sensing.

The self-assembly of peptide-functionalized GNPs induced by chelation of carboxylate groups by metal ions, such as Pb^{2+}, Cd^{2+}, Cu^{2+} or Zn^{2+}, has been investigated.[32] GNPs were formed by *in situ* reduction by tyrosine and the tripeptide H_2N-Leu-Aib-Tyr-OMe was attached to the GNP surface. In the presence of sodium hydroxide, the peptides were hydrolysed to sodium carboxylate. When heavy metal ions were added to the peptide-GNPs, self-assembly occurred instantly and gave a colour change from red to blue, due to the formation of a chelate complex. The whole process takes ca. 15 min to complete (Figure 5) and be reversed by adding concentrated alkaline EDTA solution. The study showed that this self-assembly was only driven by chelation, and not affected by pH or salt concentration.

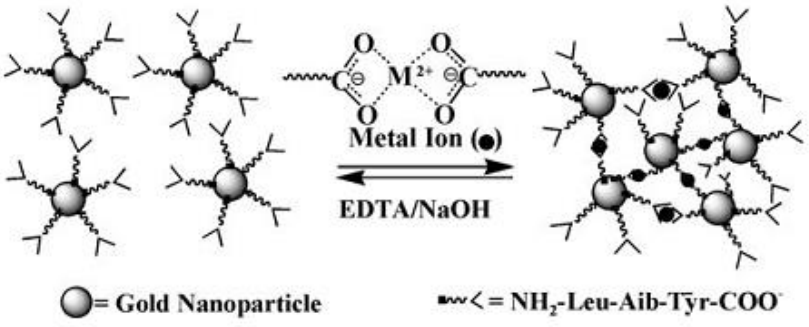

Figure 5. Reversible self-assembly of carboxylated peptide-GNPs in the presence of metal ions.[32] Reproduced with permission © Wiley-VCH, 2008.

4. Applications of Peptide-Functionalized Gold Nanoparticles

4.1 Detection

Peptide-functionalized GNPs have unique optical and electronic properties and their assembly can be triggered by changes in their local environment. Increasingly, studies have been performed to apply these properties in the biomedical area, such as in the detection of metal ions, enzymes and antibodies.

In the detection of heavy metal ions, several studies have appeared in the literature since 2007. Si *et al.*[33] developed the first peptide-functionalized GNPs to detect Hg^{2+} ions in solution. In this work, peptide-GNPs stabilised by H_2N-Leu-Aib-Tyr-OMe were prepared. The UV-Vis spectrum of the peptide-GNPs solution showed an absorbance peak at 527 nm, but after adding Hg^{2+} ions, another peak at wavelength ca. 670 nm was observed. This was accompanied by a solution colour change from red to purple (Figure 6). When alkaline EDTA solution was added, the purple colour turned back to red. This method can detect Hg^{2+} ions in solution at concentrations above 4 ppm, either by the naked eye or by UV-vis spectroscopy.

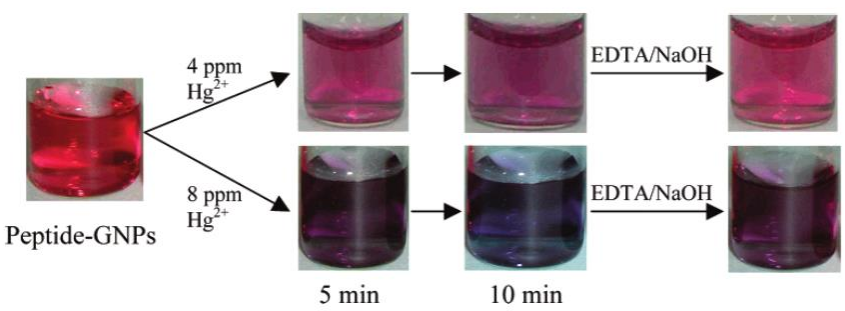

Figure 6. Detection of Hg^{2+} ions using a peptide-GNP solution.[33] Reprinted with permission from S. Si, A. Kotal and T. K. Mandal, J. Phys. Chem. C, 2007, 111, 1248-1255. Copyright 2007 American Chemical Society.

Slocik and co-workers[34] demonstrated another peptide-functionalized gold nanoparticle (PFN) system as a colorimetric sensor for various metal ions (Co^{2+}, Hg^{2+}, Pb^{2+}, Pd^{2+} and Pt^{2+}). In a one-pot process in HEPES buffer, the peptide DYKDDDDKPAYSSGPAPPMPPF reduced $AuCl_4^-$ and coated the surface of the resulting GNPs producing stable and multifunctional GNPs in solution. When the PFNs complexed with different metal ions, a reproducible and specific surface plasmon resonance (SPR) trace as well as a colourimetric response was shown for each metal ion (Figure 7).

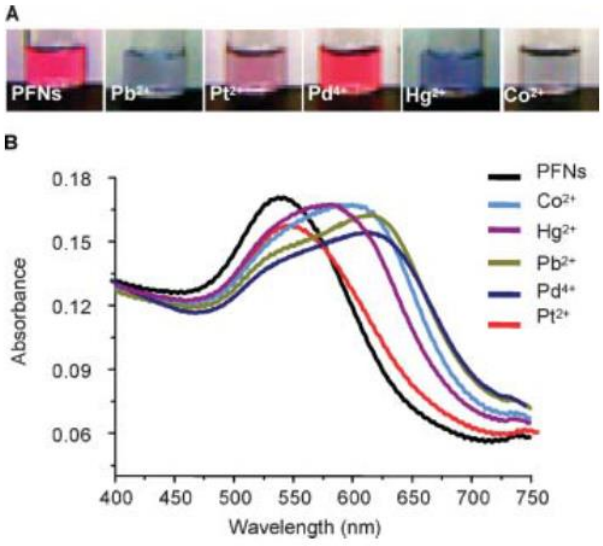

Figure 7. Response of peptide-functionalised gold nanoparticles (PFNs) to various metal ions. (A) photographs of PFN solutions after additon of various metal salts; (B) UV/Vis spectra corresponding to the photographs in (A).[34] Reproduced with permission © Wiley-VCH, 2008.

Wang *et al.*[35] studied β-amyloid peptide ($A\beta_{1\text{-}16}$)-functionalized GNPs as a colourimetric indicator for Zn^{2+}. The peptide $A\beta_{1\text{-}16}$ (DAEFRHDSGYEVHHQK) was linked to the gold surface through biotin-streptavidin chemistry. β-Amyloid peptide aggregation in the presence

of Zn^{2+} was confirmed by UV-vis spectroscopy and TEM. This aggregation precess can be reversed when EDTA is added to the solution. The mechasim of this colourimetric detector is based on the chelation between the β-amyloid peptide and the metal ion Zn^{2+}. Later in 2012, Wang *et al.*[36] discussed another colourimetric assay for detecting Pb^{2+} in presence of living cells based on CALNN and glutathione (Glu-Cys-Gly) functionalized GNPs. CALNN was used as a stablizer for the GNPs under physiological conditions, while glutathione was used as the sensor element as it can react with Pb^{2+}. In both aqueous solution and in the presence of HeLa cells, metal ions including Zn^{2+}, Cu^{2+}, Fe^{2+}, Hg^{2+} and Pb^{2+} were added separately to GNP solutions. The results indicated that the CALNN and GSH bifunctionalized GNPs have a high selectivly for Pb^{2+}. In the living cell experiment, the colourimetric assay could detect down to 2.9 fmol of Pb^{2+} per cell.

A peptide-functionalized GNP as a sensing probe for detecting in parallel mixed metal ions, such as Cd^{2+}, Ni^{2+} and Co^{2+}, has been developed.[37] CALNNDHHHHHH contains a biostable sequence as well as a metal ion sensing sequence (histidine (H) is known to bind certain metal ions via the imidazole ring). The designed peptide-functionalized GNPs were highly dispersed in buffer solution, however they were found to aggregate in the presence of Cd^{2+}, Ni^{2+} and Co^{2+}. The colour of the peptide-GNP probe gradually changed from red to purple or blue. A linear relationship between the concentration of each metal ion and the ratio of absorbance at wavelengths 600 nm and 520 nm (A_{600}/A_{520}) was found. The colourimetric response of Cd^{2+} was more obvious than Ni^{2+} and Co^{2+} and the detection limit was as low as 0.05 μM. The method is simple, quick and accurate for real samples which contain mixtures of various metal ions.

Many enzymes hydrolyse peptide bonds and thus can be used as a starting point to design a detection method for targeted enzymes. In 2008, Zhen *et al.*[38] reported a simple peptide-GNP

system to detect thrombin proteolytic activity. The peptide attached to the GNPs has the sequence GLACSGFPRGRW; and in the presence of thrombin, a serine protease, the R-G amide bond is cleaved. After centrifugation, strong fluorescence was found in the supernatant because of the tryptophan residue. As shown in Figure 8, the success of the cleavage can be confirmed by strong fluorescence of the GRW fragment. From the experimental data, a linear relationship between the concentration of thrombin and fluorescence intensity was found. This method can easily be applied to real blood samples to detect thrombin in one hour.

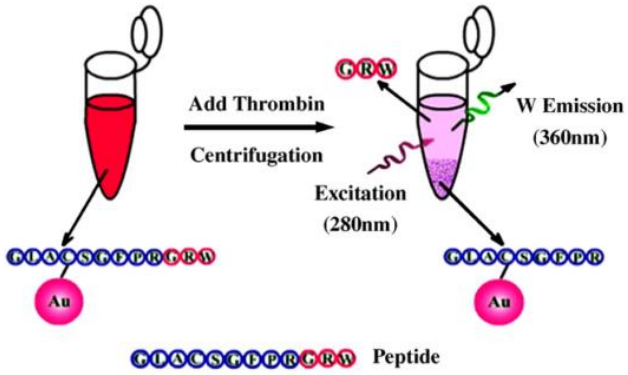

Figure 8. A peptide-GNP-based thrombin assay. The peptide covalently bound to the GNPs is cleaved at a specific site by thrombin. The GRW fragment so produced migrates to the supernatant and can be detected.[38] Reproduced with permission © Elsevier, 2008.

A colourimetric detection of the matrix metalloproteinase matrilysin (MMP-7) based on JR2EC-functionalized GNPs has been described.[39] GNPs were modified through the cysteine in the middle of the JR2EC sequence (NAADLEKAIEALEKHLEAKGPCDAAQLEKQLEQAFEAFERAG), via a thiol-gold linkage. MMP-7 can recognize and cleave two sites in JR2EC, Ala-Leu and Gln-Leu, resulting in a reduction in peptide size and overall net charge. The GNPs responded to this cleavage by aggregation, a localized surface plasmon resonance (LSPR) shift and a colour

change from red to blue. Control experiments were undertaken to verify the aggregation of GNPs was only because of the digestion of JR2EC by MMP-7, not because of chelation in the presence of metal ions Zn^{2+} and Ca^{2+}. As the level of MMP-7 in the salivary gland of cancer patients is higher (ca. >5 nM) than in healthy patients and the assay has a detection limit as low as 5nM, it shows promise as a diagnostic tool for salivary gland cancer. The JR2EC peptide was further used to probe Zn^{2+}-protein-chelant interactions.[40] The presence of chelating agents modulates the interaction between JR2EC and Zn^{2+}, giving profound effects on the LSPR band of the GNP. The system thus represents a sensitive detection system for Zn^{2+} binding species, which are prevalent in nature.

Gupta *et al.*[41] reported a one-step kinase assay involving two different functionalized 20 nm GNPs. The GNPs were modified with either the peptide Ac-IYGEFKKKC, which is a Src-kinase enzyme substrate or with anti-phosphotyrosine antibodies (Figure 9). When nanomolar concentrations of v-Src kinase and ATP were incubated with both types of GNPs, they changed from well-dispersed to aggregated. Since both kinase and ATP have to be added to the gold solution to cause the change, this method can be applied to specific drug screening if it involves inhibition of kinase activity.

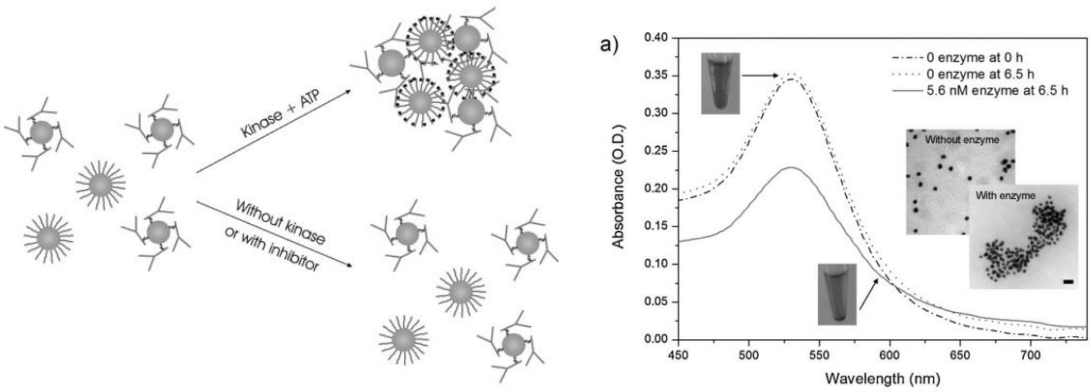

Figure 9. A peptide-GNP aggregation immunoassay for kinase detection.[41] Reproduced with permission © Wiley-VCH, 2010.

Multivalent labelled fluorescence-quenched GNP probes for the detection of proteolytic activity *in vivo* have also been developed.[42] A near-infrared fluorophore (Quasar 670) and quencher (BHQ-2) were covalently attached to protease substrates bearing a Cys at the C-terminus for conjugation to GNPs. Protease activity cleaved the peptide substrate, releasing the dye from the GNP surface giving quantifiable fluorescence. The self-assembled GNP probes were found to exhibit high image contrast in a tumour phantom model, and to have a long circulation time ($t_{1/2}$>4 h) *in vivo*. This study shows that multivalent labelled GNP probes have great potential application in detection and therapeutic delivery.

Recently, GNPs have been developed as colourimetric immunosensors. Yuan *et al.*[43] developed glutathione (GSH)-functionalized GNPs for detecting neurofenin3 (ngn3), which is essential in the development of islet cells. Previous studies had shown that mice that cannot produce ngn 3 fail to generate pancreatic endocrine cells and subsequently die from diabetes.[44, 45] Based on this work, the development of new methods to detect ngn3 is potentially very useful. Anti-ngn3 antibody was bound to GSH-GNPs through electrostatic interactions to form GNP-Ab. In the presence of either ngn3 or NaCl, the UV-vis absorbance was similar to that of GNP-Ab alone, however when both ngn3 and NaCl were added, a broad new band appeared at high wavelength corresponding to GNP aggregation (Figure 10). The positively charged ngn3 and negatively charged anti-ngn3 combine to neutralize the surface charge, and the neutral nanoparticles aggregate in salt solution. This is the first example of a label-free colourimetric assay to detect ngn3 easily by optical absorption spectra.

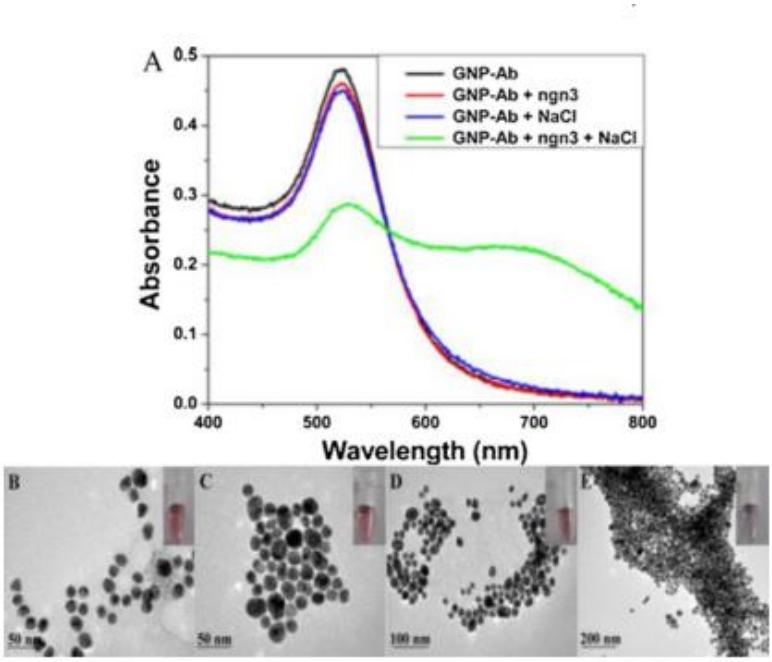

Figure 10. Antibody-functionalised GNPs for detecting neurofenin3 (ngn3). (A) Absorption spectra of Anti-ngn3-GNPs in the presence of no additive, ngn3, NaCl and ngn3+NaCl; (B–E) corresponding TEM images plus photos ((B): no additive; (C): +ngn3; (D): +NaCl; (E): +ngn3+NaCl).[43] Reproduced with permission © Elsevier, 2011.

In 2012, Saxena *et al.*[46] discovered a novel approach to detect bluetongue virus (BTV)-specific antibodies based on multiple antigenic peptide (MAP)-functionalized GNPs. In this work, an antigenic peptide was designed based on the region of the BTV structural protein VP7. This protein was chosen as it shows high sequence homology amongst the serotypes. Gold nanoparticles were decorated with antigenic peptides in a format with a cysteine core and four arms linked through Di-Fmoc-Lys, to amplify the sensitivity. When GNPs labeled with MAP met the specific BTV antibodies, they became aggregated resulting in a colour change from pink to violet. This novel approch using MAP fuctionalized GNPs has the advantage of minimizing the risk of infectious organisms and highly specific targeting to

BTV antibodies at the same time. A peptide-GNP system for detection of botulinum neurotoxin (BoNT) was also developed.[47] GNPs were surface functionalised with a peptide cleavage site for Botulinum A light chain (BoLcA), bearing a C-terminal biotin moiety. In the presence of streptavidin-Alexa488 complex, energy transfer between the dye and the GNP resulted in fluorescence quenching. Addition of BoLcA cleaved the peptide, releasing the Alexa conjugate from the nanoparticle surface and swtiching on fluorescence. BoClA could be detected at concentrations as low as 1pM using this approach.

A GNP system that could detect interaction between the estrogen receptor alpha subtype (hERα) and agonist ligands was reported.[48] The GNPs were functionalized with peptides that contained a section of SRC-1, which is a co-activator for a nuclear receptor. Aggregation of GNPs in solution only occurs in the presence of an agonist ligand, as confirmed by a red shift of the SPR absorption band and a colour change from red to blue (Figure 11). This assay gives a better understanding of ligand agonist/antagonist activity compared to former assays and is applicable for screening in drug discovery.

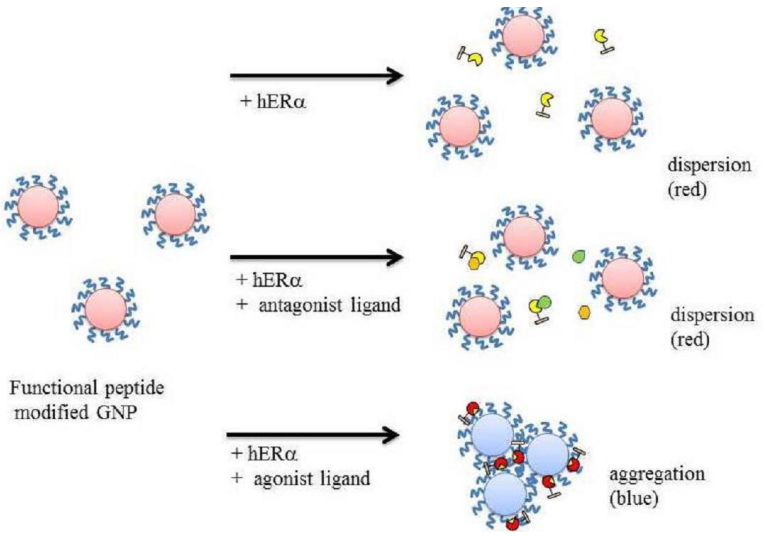

Figure 11. SRC-1 peptide-functionalised GNPs for detection of the interaction between estrogen receptors and agonist ligands.[48] Image re-used under Creative Commons Attribution Licence (CC-BY 3.0).

Detection of proteins by double-recognition peptide-aptamer-functionalized GNPs has been described recently.[49] The binding sequences of proteins p53 and p14, which form a ternary complex with oncoprotein Mdm2, were attached separately to the surface of GNPs. When Mdm2 was added to mixed solutions of the two GNPs, a large shift in LSPR and an associated colour change from red to purple was observed. A remarkably low detection limit of 20nM was demonstrated, with a linear response in the range 30-50nm. No aggregation was observed in the presence of BSA (even at physiological concentration), or if only one of the peptide aptamer-GNPs was present. A GNP protein-detection assay employing a smartphone as detector has also been described recently.[50] Protein-detecting gold nanorods have been incorporated into a paper-based biodiagnostic device.[51] A peptide that binds human troponin 1, a cardiac biomarker, was identified by phage display and attached to the surface of the gold nanorods via a C-terminal Cys. The peptide-GNPs were absorbed into paper to create a bioplasmonic device; the detection limit of the target protein troponin 1 was 35.3 pg/ml, one order of magnitue lower than an analogous Ab-GNP bioplasmonic device. Furthermore, the peptide-GNP system showed greater stability and better sensitivity in physiological media than the antibody-modified GNPs.

A dot-blot GNP-based immunoassay for detecting β-amyloid peptide ($A\beta_{1-42}$) was created by Wang and co-workers.[52] The C-terminal antibody of $A\beta_{1-42}$ was immobilized on a nitrocellulose membrane. On top of this, biotin- and N-terminal $A\beta_{1-42}$ antibody-cofunctionalized GNPs (Ab16-GNP) plus streptavidin-functionalized GNPs (SA-GNP) were

added. These nanoparticles bind together through biotin-streptavidin interaction, amplifying the detection signal. In the presence of $A\beta_{1-42}$, a does-dependent positive dot-blot immunoassay was clearly observed on the fixed nitrocellulose membrane (Figure 12). This detection method is easy and efficient for complex biosamples and can detect $A\beta_{1-42}$ down to 50 pg mL^{-1} in solution.

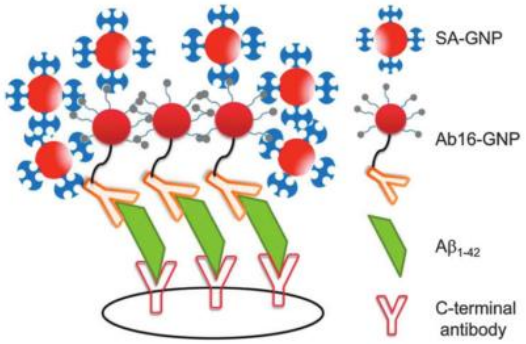

Figure 12. A GNP-based dot-blot immunoassay for detecting the β-amyloid petide $A\beta_{1-42}$.[52] Reproduced with permission © Royal Society of Chemistry, 2012.

In 2014, Chandrawati *et al.*[53] demonstrated a label-free detection method for blood coagulation factor XIII activity based on the optical and electronic properties of GNPs. Factor XIII is active in the presence of thrombin and Ca^{2+} and it catalyses the formation of an amide bond between the side chains of the amino acid residues Gln and Lys. GNPs were functionalized separately with two different peptides, CALNNGQG and CALNNGKG. If factor XIII is present, the Gln-Lys bond forms an intermolecular crosslink between the two types of GNPs and aggregation occurs. A red shift of the surface plasmon resonance (SPR) absorption band confirmed the aggregation and a solution colour change from red to blue was observed (Figure 13). A linear relationship between the concentration of Factor XIII and the

difference of the maximum absorbance peak ($\Delta\lambda_{max}$) was observed and the detection limit was down to 0.01U mL^{-1}. This provides a label-free and very sensitive approach to detect the activity of Factor XIII.

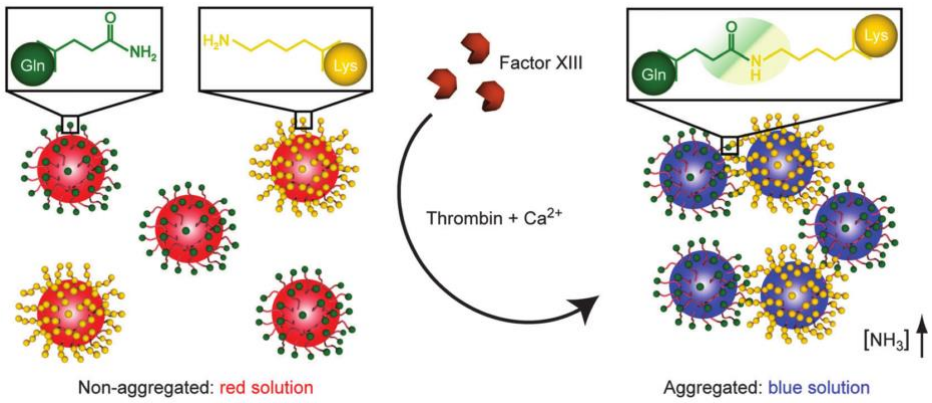

Figure 13. Label-free detection of blood coagulation Factor XIII activity by the controlled assembly of peptide-GNPs in the presence of thrombin and Ca^{2+}.[53] Reproduced with permission © Royal Society of Chemistry, 2014.

4.2 Targeted Drug Delivery and Cellular Uptake

In recent years, peptides have been used in a variety of biomedical applications, including as targeting probes, drug carriers and synthetic vaccines, because of their small size, biocompatibility, cell-penetrating ability, easy chemical synthesis and modification.[5, 6] Chan *et al.*[54] found that GNPs with diameters between 20-60 nm have the highest uptake in HeLa cells. Also, it was found that some peptides, known as cell-penetrating peptides (CPPs), can be uptaken specifically by certain cell organelles. They can be conjugated to an anti-cancer drug and used as a drug carrier. Functionalization of gold nanoparticles (GNPs) with a cell-

penetrating peptide has been performed with the aim of improving the efficiency of living cell uptake.

In 2005, Fuente and Berry[55] attached the HIV-derived CPP Tat (GRKKRRQRRR) to GNPs in order to develop a system that was able to target the cell nucleus.. The GNPs were firstly synthesized by reduction of $AuCl_4^-$ solution in the presence of tiopronin which has a thiol end group. Secondly, Au@tiopronin acid groups and Tat peptide amine groups were conjugated via EDC/NHS coupling to give Au@Tat nanoparticles. This strategy has been also used to develop water-soluble and biocompatible fluorescent quantum dots which can translocate to the nucleus.[56] Human fibroblast cells (HTERT-BJ1) were used to test the biocompatibility of Au@tiopronin and Au@Tat and cell uptake was investigated by TEM. These results indicate that this Tat peptide can transfer the nanoparticles into the cell nucleus. Without the peptide functionalization, Au@tiopronin nanoparticles could not penetrate the cell membrane and target the cell nucleus, proving the cell-penetrating ability of Tat peptide. This work has many potential applications in cancer therapy, for example as a carrier for drug delivery. However, the ratio of Tat/tiopronin on the surface is about 1:50 which is low and makes it hard to quantify Tat loading. In related work, Tat-GNPs were used to probe the spatio-temporal uptake of nanoparticles by HeLa cells, using dual wavelength view darkfield microscopy.[57] Uptake was shown to be by energy dependent endocytosis; interestingly, Tat-GNPs were passed on to daughter cells by mitosis. Tat has also been conjugated to gold nanostars to create ultra-bright imaging agents for tracking mesenchymal stem cells (MSCs) after implantation in mice.[58] These peptide-gold nanostar clusters gave a stronger and slower decaying intracellular signal than the commercial cell tracking agent Q-Tracker (a peptide-conjugated quantum dot).

In 2008, Sun *et al.*[59] utilised a CPP-modified CALNN derivative ($CALNNR_8$) to prepare GNPs that could target intracellular components. In this study, GNPs of three different sizes (13nm, 30nm, 60nm) were synthesized by the Frens-Turkevich method.[3, 4] The peptide-capped GNPs were then prepared by a one-step gold-thiol reaction. The ratio of the $CALNNR_8$ to CALNN on the surface of the GNPs was determined to be 1:9 respectively. After incubation with HeLa cells, it was found that the peptide-GNPs had translocated into the cell nucleus. However, if the system was modified to only contain $CALNNR_8$, the GNP complex did not reach the nucleus and it was found to remain in the cytoplasm. It was also found that the size of the gold particles can affect cellular internalization. Larger GNPs (60 nm) were internalized to a lesser extent by HeLa cells compared to smaller (13 nm and 30 nm) nanoparticles. The mechanism behind this is still unclear and needs to be investigated further. Penetratin, another example of a CPP, was employed as a ligand to enhance passage of gold nanostars across the blood-brain barrier (BBB) for photothermal disruption of β-amyloid fibrillation.[60] A derivative of maurocalcine (MCa), an alternative CPP, enabled enhanced uptake in certain cancer cell lines when attached to GNPs surface, but not in others.[61] Interestingly, the MCa derivative, unlike most CPPs, is charge neutral, indicating that its cell-penetrating mechanism may not be electrostatic.

A GNP system for targeting tumour vasculature has been reported by Shukla *et al.*[62]. Arg-Gly-Asp (RGD) peptide-functionalized dendrimer-entrapped gold nanoparticles (AuDENPs) which can be taken up by $\alpha_V\beta_3$ integrin-expressing cell lines were prepared. The $\alpha_V\beta_3$ integrin is an important marker of the neovasculature and is normally found during tumour angiogenesis; without it, tumours cannot grow beyond 1-2 mm in size.[63] AuDENPs with a mean diameter of 3.0 nm were synthesized.[64] Human dermal microvessel endothelial cells (HDMEC) and human vascular endothelial cells (HUVEC) were used to examine the binding

ability of Au DENPs and confocal microscope results confirmed the internalization of gold in the integrin-expressing cells. Given that the RGD peptide has a high affinity to $\alpha_V\beta_3$ integrin, the RGD-functionalized GNPs can be used as a drug carrier system to delivery anti-cancer drugs or pro-apoptotic peptides.[65] However, the interaction between linear RGD peptides and $\alpha_V\beta_3$ integrin is often weak and the utility of individual ligands is limited for efficient tumour targeting. Arosio *et al.*[66] improved this approach by using cyclic RGD derivatives to functionalise GNPs. A short poly(ethylene glycol) (PEG) was used as a spacer to combine the cRGD and the GNPs, and to enhance the stability of the nanoparticle system. Experimental results with PC-3 prostate cancer cells showed that cRGD-conjugated GNPs had enhanced affinity for $\alpha_V\beta_3$ integrin compared with the unconjugated system.

Another cyclic RGD (RGDfK) peptide-functionalized GNP system has been reported in which Multiphoton-Absorption-Induced Luminescence (MAIL) was used to monitor GNP uptake into cells.[67] HUVECs were incubated with cyclic RGDfK- and linear RGD (GRGDSP)-functionalized GNPs. MAIL showed that the number of GNP-RGDfK conjugates targeted to HUVECs was an order of magnitude higher than GNP-GRGDSP. MAIL imaging also demonstrated that the mechanism of uptake of the GNP-RGDfK conjugate into cells involves $\alpha_V\beta_3$ integrin-mediated endocytosis which is a specific binding event. Ghosh *et al.*[68] synthesized GNPs coated with a short peptide that can promote intracellular delivery of β-galactosidase (β-gal), which is a 465 kDa membrane-impermeable protein (Figure 14). The peptide ligand was attached to the end of a spacer containing a hydrophobic domain adjacent to the nanoparticle surface and a short, passivating, oligoethyleneglycol sequence. Fiammengo's group[69] similarly prepared peptide-functionalised GNPs where a toxic *N*-methyl-D-aspartate (NMDA) receptor targeting peptide, conantokin-G (conG), was tethered at the end of an alkyl-PEG spacer unit in a mixed monolayer. The peptides could be

conjugated selectively to the end of the alkyl-PEG spacer and thus gave maximum receptor binding, while use of a heterobifunctional PEG without an alkyl sequence also resulted in some direct peptide attachment to the gold surface.

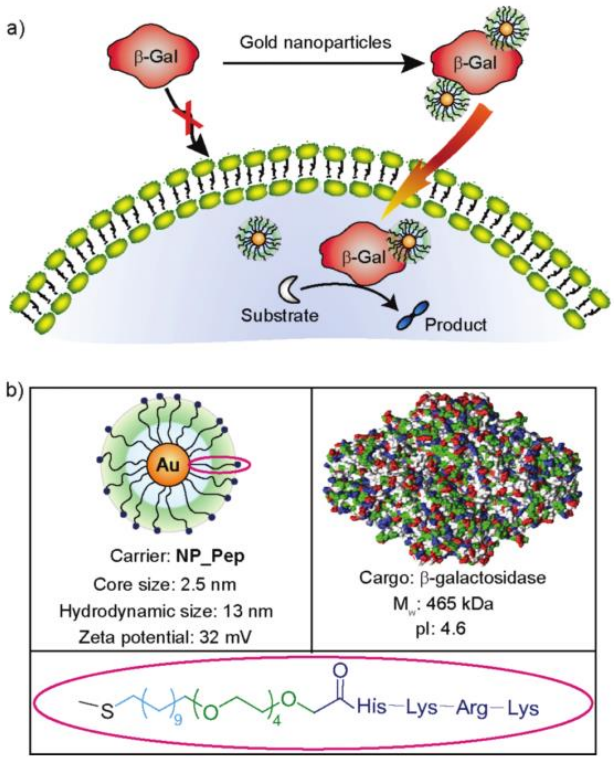

Figure 14. Short peptide-coated GNPs for intracellular delivery of β-galactosidase (β-gal): (a) Schematic showing intracellular delivery mechanism; (b) structure and properties of the GNP, β-gal and the peptide ligand.[68] Reprinted with permission from P. Ghosh, X. Yang, R. Arvizo, Z.-J. Zhu, S. S. Agasti, Z. Mo and V. M. Rotello, J. Am. Chem. Soc., 2010, 132, 2642-2645. Copyright 2010 American Chemical Society.

Amphiphilic peptide-functionalized GNPs which can encapsulate a cargo and release it following a biostimulus have been described.[70] An amphiphilic peptide containing a hydrophobic core of repeating units $(PPG)_n$ (n=3, 5, 8 or 10) and a hydrophilic exterior sequence of four aspartic acids (D) was used. The hydrophobic dye BODIPY was

encapsulated into the particles as a drug model; the GNP-$(PPG)_5$ showed the highest loading capacity due to the largest hydrodynamic radius. Based on this, a thrombin cleavable peptide $DDDD(PPG)_2LVPRGS(PPG)_3GC$ ($(PPG)_5$') was designed. In the presence of thrombin, Arg-Gly (R-G) amide bonds are cleaved. A short peptide DDNNLAC and $(PPG)_5$' were used at a ratio of 1:1 to form a mixed monolayer on the gold nanoparticle surface and then the hybrid particles were used to encapsulate BODIPY. Without thrombin, BODIPY was released slowly while in the presence of thrombin it was released rapidly. This novel stimulus-release drug delivery model has the potential to be applied to cancer cells, while the use of other proteases to replace thrombin can diversify the field of application.

Yang *et al.*[71] investigated the effect of surface chemistry of different peptide-functionalised GNPs on their interaction with cells. The peptides contained a gold-binding cysteine, a hydrophobic spacer of four alanine residues and end groups with different charge status, such as arginine (P1), lysine (P5), glutamic acid (P2), serine (P3) and tryptophan (P4). Stability experiments showed that only the negatively charged glutamic acid-ended peptides prevented GNPs from aggregating. By changing 5-10% of the end group amino acid residues, various P2-P3 and P2-P4 mixed-functionalized GNPs were synthesized and their cellular uptake properties were studied. It was shown that mixed peptide 95P2P4 (95% P2 and 5% P4) functionalized-GNPs had enhanced cellular uptake properties. This enhancement was thought to be due to the ability to interact with cellular membranes afforded by the aromatic amino acid tryptophan (P4). Terminal amino acids were similarly shown to affect the toxicity of glutathione-modified GNPs.[72] Bartczak *et al.*[73] studied the cellular uptake properties and exocytosis behaviour of two different types of peptide-GNPs in human endothelial cells (HUVECs). The first peptide KATWLPPR interacts strongly with endothelial-expressed receptor Neuropilin 1 (NRP-1) as an inhibitor, while the second peptide KPRQPSLP does not

interact with surface-bound receptors. Both peptides were attached to oligoethyleneglycol (OEG) modified GNPs through EDC/NHS chemical conjugation. Endothelial cell experiments showed that both peptide-GNPs can be taken up in greater numbers compared to bare GNPs. However, NRP-1 non-binding GNPs are retained by cells while the inhibitor-GNPs are progressively exocytosed.

4.3 Delivery of Anti-cancer peptides

In vitro experiments have shown that some peptides have the ability to kill cancer cells and inhibit tumour growth. These anti-cancer peptides can be used as therapeutics and a range of systems for their targeted/controlled delivery have been studied. One such approach is the functionalization of GNPs with a targeting peptide, which has been used to deliver anti-cancer peptides specifically to tumour cells.

In 2010, Chanda *et al.*[74] conjugated analogues of the peptide bombesin (BN) to GNPs. Bombesin is a gastrin-releasing peptide (GRP) that can specifically target cancer cell receptor sites. It is known that BN peptides have a high affinity for GRP receptors which are overexpressed in breast, prostate and lung carcinomas. Human prostate tumour PC-3 cells were used to evaluate the GRP receptor binding affinity of BN-functionalized GNPs. The higher the degree of BN peptide on the GNP surface, the higher was the cell binding affinity, as shown by lower IC_{50} values. A multi-functionalized GNP system that contains both BN and a therapeutic peptide has also been developed.[75] RAF peptide inhibits *in vivo* the kinase Rb-Raf-1 and thus prevents cell proliferation. GNPs of 20 nm diameter were synthesized by the sodium citrate reduction method,[4] and these were then conjugated with BN and RAF. The multi-functionalized GNP system was found to penetrate HeLa cells which overexpress GPRr,

while it was not taken up by SHSH-5Y cells which do not overexpress the same receptor (Figure 15). The mechanism of internalization into HeLa cells is still under investigation.

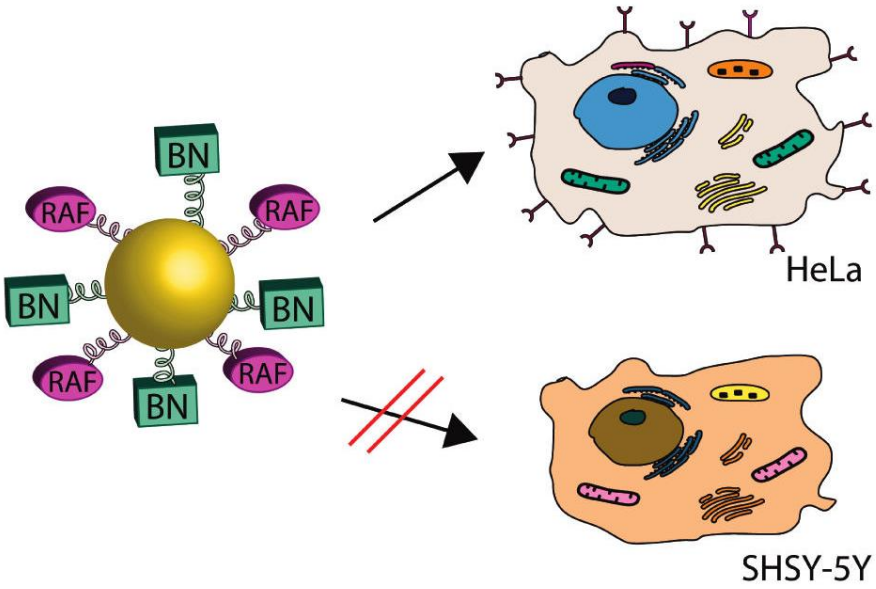

Figure 15. Multifunctionalization of gold nanoparticles with a targeting peptide (bombesin; BN) and an antitumoral peptide (RAF).[75] Reprinted with permission from L. Hosta-Rigau, I. Olmedo, J. Arbiol, L. J. Cruz, M. J. Kogan and F. Albericio, Bioconjug. Chem., 2010, 21, 1070-1078. Copyright 2010 American Chemical Society.

Further work involving BN as a cancer-targeting ligand for GNPs has revealed stark differences between in vitro and in vivo behaviour.[76] [67]Ga-radiolabelled GNPs either with or without a surface-bound BN derivative were prepared and their uptake into GRPr-positive human pancreatic cancer cells was investigated. Remarkably raid and efficient uptake (25% after 15 min) of GNPs bearing a BN derivative was observed. Mechanistic studies revealed that uptake most likely occurs via active pathways (phagocytosis and/or endocytosis). However, follow-up experiments in mice indicated high uptake of BN-GNPs into organs including the liver, spleen and lungs with low uptake (3.3-3.7% after 24h) in tumour tissue.

Furthermore, GRPr blocking experiments had no effect on uptake, indicating that GNPs are being uptaken in tumours by a passive (EPR) mechanism. These results highlight the difficulties of translating *in vitro* nanoparticle cancer targeting approaches to success *in vivo*.[77]

In 2012, Kumar *et al.*[78] developed novel small GNPs (2 nm) functionalized with both a therapeutic peptide (p12) and a targeting peptide (CRGDK). The targeting peptide is known to bind selectively to Nrp-1 receptors which are overexpressed in many tumour cells. Through receptor-mediated internalization, targeting peptide-functionalized GNPs can translocate into the cell and the nucleus. At the same time, the therapeutic peptide p12 binds to MDM2 and MDMX proteins leading to the expression of tumour suppressive protein p53, which limits the expression of tumour genes thus causing cell apoptosis.[79] The same GNP synthesis method as is shown in Figure 1 was used, giving small Au@tiopronin to which were added peptide p12, CRGDK or both peptides together. The targeting peptide was shown to enhance the cellular uptake of the gold nanoparticles with the therapeutic peptide payload. A multifunctional GNP system with the same targeting peptide (CRGDK) and a platinum (IV) drug for prostate cancer treatment was also reported.[80] The anti-cancer targeting nanocarrier had improved efficiency of intracellular uptake compared to non-targeting analogues and enhanced cytotoxicity (8.25 times more cytotoxic than non-targeting Pt(IV)-modified GNPs).

Ma *et al.*[81] and Chen *et al.*[82] have reported two similar systems which use a pro-apoptotic peptide $(KLAKLAK)_2$ to functionalize GNPs for enhanced cancer treatment (Figure 16). The cytotoxic KLA peptide disrupts the mitochondrial membrane, resulting in release of cytochromes and induction of apoptosis. In Ma's system, GNPs was firstly stabilized with a biotinylated CALNN-based peptide (biotin-NNLACCALNN-COOH), then a tetrameric streptavidin layer, and lastly a biotinylated KLA peptide. Chen's group used only KLA

peptide (referred to as pro-apoptotic peptide, or PAP) to functionalize gold nanoparticles. In both systems, the KLA peptide-functionalized GNPs displayed greatly enhanced activity compared to free KLA peptide. Derivatives of KLA peptides with better cell penetrating ability were identified using prediction software, the best candidate being WKRAKLAK.[83] This was conjugated to GNPs of different size and shapes (spheres and rods) via a lipoic acid spacer. Strong influence of GNP size and shape on cancer cell uptake and cytotoxicity were observed. For example, smaller nanospheres were uptaken more efficiently and were more cytotoxic, while nanorods were more hemolytically active than nanospheres. These results demonstrate the importance of GNP size and shape on activity.

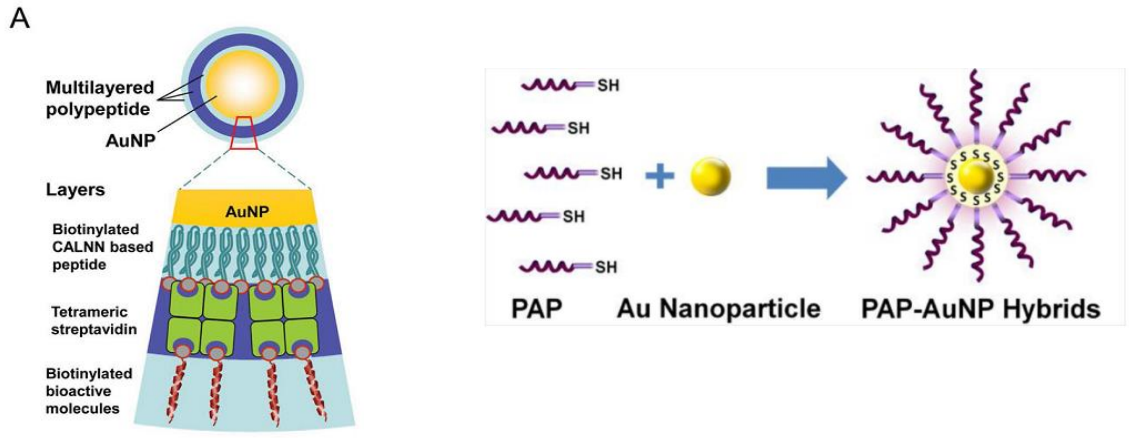

Figure 16. GNP systems for the delivery of anti-cancer peptide KLA: A) a gold nanoparticle core with multi-layered presentation of KLA peptide.[81] B) GNPs directly functionalized with the pro-apoptotic peptide (PAP) KLA.[82] Reproduced with permission © Royal Society of Chemistry, 2013.

4.4 Oligonucleotide Delivery and Regulation of Gene Expression

Cationic macromolecules have the ability to bind and condense oligonucleotides and thus have been the result of intense investigation as non-viral vectors for gene and RNA delivery. In particular, poly(ethyleneimine) (PEI), PEGylated poly(L-lysine) (PEG-PLL), PAMAM dendrimers and a cationic lipid known as Lipofectamine® have been the most commonly studied oligonucleotide vectors. Gold nanoparticles have been employed in some studies as non-toxic delivery platforms for cationic vectors, in conjugation with cell-penetrating peptides or other targeting moieties for enhancing transfection of oligonucleotides.

Franzen and Liu employed streptavidin-conjugated gold nanoparticles as a multifunctional platform for the delivery of a biotinylated antisense oligonucleotide, together with various biotinylated targeting peptides[84]. It was found that targeting peptide-conjugated GNPs displayed enhanced antisense activity roughly two-fold relative to Lipofectamine® (LF) control, however only in the presence of free LF. The presentation of the oligonucleotide on the GNP surface may expose it to harsh conditions once inside the endosome, leading to its degradation. The presence of free LF was suggested to ameliorate this, possibly by allowing the oligonucleotide to escape the endosome and access the nucleus. Kataoka and coworkers employed cyclic-RGD (cRGD) as a targeting ligand for GNP-mediated delivery of siRNA to silence an HPV-derived oncogene[85]. A cRGD-PEG-PLL-lipoic acid construct was complexed with the siRNA sequence then the complex was immobilised on citrate-GNPs. The presence of cRGD both enhanced gene silencing *in vitro* and decreased tumour size in an *in vivo* (mouse) model. Cationic polypeptide-conjugated GNPs were prepared in a single-step process whereby the polypeptide acts both to reduce $HAuCl_4$ and stabilise the resulting GNPs[86]. Poly(L-lysine) (PLL)-containing polypeptides were able to bind a GFP plasmid DNA sequence and high levels of transfection were demonstrated *in vitro* after 10 days. At earlier times, however, transfection efficiency was lower than analogous systems without the

GNP platform. This was attributed to the observed significant GNP clustering at earlier time points, which was also accompanied by higher cytotoxicity of GNP-polypeptide constructs.

Cell-penetrating peptides (CPPs) have been employed to enhance uptake of GNP non-viral gene transfer vectors. A novel zwitterionic cell penetrating pentapeptide was conjugated to GNPs that also carried a linearised plasmid encoding for a brain-derived neurotrophic factor (BDNF)/mCherry fusion protein, for transfection of mesenchymal stem cells (MSCs)[87]. Transfection efficiency as measured by mCherry expression was massively enhanced compared to LF control. MSC transfection was also assisted by an antimicrobial CPP from lactoferrin[88]. This CPP, known as PEP, was co-immobilised with PEI onto GNPs and used to deliver a luciferase reporter gene to MSCs. High transfection efficiency both *in vitro* and *in vivo* (the latter using pDNA-VEGF as a reporter) was observed in the presence of PEP-GNPs; *in vitro* transfection was around 100 times higher than that of PEI control. Furthermore, high antimicrobial activity of the PEP-GNP conjugates was demonstrated *in vitro* and *in vivo*. Parang et al. employed the cyclic decapeptide $(WR)_5$ both to reduce Au^{3+} and cap in-situ formed GNPs[89]. These were shown to deliver a non-targeting siRNA sequence to HeLa cells with high levels of uptake.

In addition to the delivery of oligonucleotides, peptide-GNPs have also been used as artificial transcription factors (TFs) to alter gene expression. Lee et al. conjugated separately to GNPs peptide sequences representing the three essential domains of natural TFs, namely a nuclear localisation signal, a DNA binding domain and an activation domain[90]. The resulting construct, named NanoScript, was co-transfected with an alkaline phosphatase (ALP) reporter plasmid into HeLa cells. ALP expression was found to be dose-dependent on NanoScript concentration, and was enhanced 15-fold relative to control only when all three TF domain peptides were present.

5. Conclusions and Outlook

In conclusion, gold nanoparticles (GNPs) can be functionalized by peptides through ligand exchange, chemical reduction and chemical conjugation methods. The attached peptides can increase the stability and biocompatibility of the GNPs. The wide range of synthetic methods available provides an opportunity to conjugate almost any biofunctional peptide to the surface of GNPs. In this review, the use of peptide-GNPs as sensitive biosensors, drug carriers, anti-cancer therapeutics and gene delivery vectors has been discussed. The rapidly increasing number of papers published in this area clearly shows the potential of peptide-GNPs in nanomedicine. There are however a number of issues that still need to be resolved, including: developing methods for precisely controlled functionalization; elucidation of mechanisms of molecular recognition on the surface of GNPs; determination of the mechanism of internalization of peptide-GNPs into cells. The long-term stability and toxicity of GNP-peptide systems also must be studied in more detail. Recent *in vivo* studies involving peptide-GNPs have not revealed any significant toxicity. Biodistribution studies in mice of CPP-functionalised GNPs indicated nanoparticle concentration in the liver and spleen but without any noticeable tissue damage[91]. Similarly, pentapeptide-GNPs (CALNN and others) concentrated in the liver following intravenous injection in rats, again without any signs of toxicity[92]. Other *in vivo* studies conducted using cyclic-RGD-conjugated nanogold tripods[93], RGD-gold nanorods[94], VEGF-receptor binding peptide-[95] and adipose homing peptide-functionalised GNPs[96] similarly did not reveal any evidence of toxicity or other adverse effects, although it should be pointed out that all these studies are relatively short-term. An *in vivo* study in mice of unfunctionalised GNPs indicated significant toxicity of nanoparticles in the size range 8-37nm however, interestingly, conjugation of immunogenic peptides to the

GNPs reduced toxicity significantly[97]. Further studies are required to investigate more fully the *in vivo* effect of peptide-functionalised GNPs.

Acknowledgement

We thank the China Scholarship Council for funding (Scholarship to JYZ).

Notes and References

1. M.-C. Daniel and D. Astruc, *Chem. Rev.*, 2004, **104**, 293-346.
2. S. Eustis and M. A. El-Sayed, *Chem. Soc. Rev.*, 2006, **35**, 209-217.
3. J. Turkevich, P. C. Stevenson and J. Hillier, *Discuss. Faraday Soc.*, 1951, **11**, 55-75.
4. G. Frens, *Nature*, 1973, **241**, 20-22.
5. J. Thundimadathil, *J. Amino Acids*, 2012, **2012**, 967347.
6. C. Borghouts, C. Kunz and B. Groner, *J. Pept. Sci.*, 2005, **11**, 713-726.
7. P. M. Tiwari, K. Vig, V. A. Dennis and S. R. Singh, *Nanomaterials*, 2011, **1**, 31-63.
8. L. A. Dykman and N. G. Khlebtsov, *Chem. Rev.*, 2014, **114**, 1258−1288.
9. S. Rana, A. Bajaj, R. Mout and V. M. Rotello, *Adv. Drug Del. Rev.*, 2012, **64**, 200-216.
10. R. M. Levine, C. M. Scott and E. Kokkoli, *Soft Matter*, 2013, **9**, 985-1004.
11. S. Si and T. K. Mandal, *Langmuir*, 2007, **23**, 190-195.
12. M. J. Hostetler, A. C. Templeton and R. W. Murray, *Langmuir*, 1999, **15**, 3782-3789.
13. A. C. Templeton, W. P. Wuelfing and R. W. Murray, *Acc. Chem. Res.*, 2000, **33**, 27-36.
14. R. Lévy, N. T. Thanh, R. C. Doty, I. Hussain, R. J. Nichols, D. J. Schiffrin, M. Brust and D. G. Fernig, *J. Am. Chem. Soc.*, 2004, **126**, 10076-10084.
15. Z. Krpetic, P. Nativo, F. Porta and M. Brust, *Bioconjug. Chem.*, 2009, **20**, 619-624.

16. C. Vericat, M. Vela, G. Benitez, P. Carro and R. Salvarezza, *Chem. Soc. Rev.*, 2010, **39**, 1805-1834.

17. S.-Y. Lin, Y.-T. Tsai, C.-C. Chen, C.-M. Lin and C.-h. Chen, *J. Phys. Chem. B*, 2004, **108**, 2134-2139.

18. R. R. Bhattacharjee, A. K. Das, D. Haldar, S. Si, A. Banerjee and T. K. Mandal, *J. Nanosci. Nanotechnol.*, 2005, **5**, 1141-1147.

19. I. Pujols-Ayala, C. A. Sacksteder and B. A. Barry, *J. Am. Chem. Soc.*, 2003, **125**, 7536-7538.

20. *US Pat.,* 20,130,123,466, 2013.

21. T. Serizawa, Y. Hirai and M. Aizawa, *Langmuir*, 2009, **25**, 12229-12234.

22. W. Xie, L. Wang, Y. Zhang, L. Su, A. Shen, J. Tan and J. Hu, *Bioconjug. Chem.*, 2009, **20**, 768-773.

23. D. Bartczak and A. G. Kanaras, *Langmuir*, 2011, **27**, 10119-10123.

24. V. Lemieux, P. H. H. M. Adams and J. C. M. van Hest, *Chem. Commun.*, 2010, **46**, 3071-3073.

25. C. Minelli, J. X. Liew, M. Muthu and H. Andresen, *Soft Matter*, 2013, **9**, 5119-5124.

26. Z. Wang, R. Lévy, D. G. Fernig and M. Brust, *Bioconjug. Chem.*, 2005, **16**, 497-500.

27. A. K. Nowinski, A. D. White, A. J. Keefe and S. Jiang, *Langmuir*, 2014, **30**, 1864−1870.

28. A. Laromaine, L. Koh, M. Murugesan, R. V. Ulijn and M. M. Stevens, *J. Am. Chem. Soc.*, 2007, **129**, 4156-4157.

29. D. Aili, K. Enander, L. Baltzer and B. Liedberg, *Nano Lett.*, 2008, **8**, 2473-2478.

30. D. Aili, K. Enander, J. Rydberg, I. Nesterenko, F. Björefors, L. Baltzer and B. Liedberg, *J. Am. Chem. Soc.*, 2008, **130**, 5780-5788.

31. D. Aili, R. Selegård, L. Baltzer, K. Enander and B. Liedberg, *Small*, 2009, **5**, 2445-2452.

32. S. Si, M. Raula, T. K. Paira and T. K. Mandal, *ChemPhysChem*, 2008, **9**, 1578-1584.

33. S. Si, A. Kotal and T. K. Mandal, *J. Phys. Chem. C*, 2007, **111**, 1248-1255.

34. J. M. Slocik, J. S. Zabinski, D. M. Phillips and R. R. Naik, *Small*, 2008, **4**, 548-551.

35. C. Wang, J. Wang, D. Liu and Z. Wang, *Talanta*, 2010, **80**, 1626-1631.

36. D. Zhu, X. Li, X. Liu, J. Wang and Z. Wang, *Biosens. Bioelectron.*, 2012, **31**, 505-509.

37. M. Zhang, Y.-Q. Liu and B.-C. Ye, *Analyst*, 2012, **137**, 601-607.

38. S. J. Zhen, Y. F. Li, C. Z. Huang and Y. F. Long, *Talanta*, 2008, **76**, 230-232.

39. P. Chen, R. Selegård, D. Aili and B. Liedberg, *Nanoscale*, 2013, **5**, 8973-8976.

40. W. C. Mak, R. Selegard, M. Garbrecht and D. Aili, *Part. Part. Syst. Char.*, 2014, **31**, 1127-1133.

41. S. Gupta, H. Andresen, J. E. Ghadiali and M. M. Stevens, *Small*, 2010, **6**, 1509-1513.

42. C. J. Mu, D. A. LaVan, R. S. Langer and B. R. Zetter, *ACS Nano*, 2010, **4**, 1511-1520.

43. Y. Yuan, J. Zhang, H. Zhang and X. Yang, *Biosens. Bioelectron.*, 2011, **26**, 4245-4248.

44. G. Gradwohl, A. Dierich, M. LeMeur and F. Guillemot, *Proc. Natl. Acad. Sci. USA*, 2000, **97**, 1607-1611.

45. S. Yoshida, A. Takakura, K. Ohbo, K. Abe, J. Wakabayashi, M. Yamamoto, T. Suda and Y.-i. Nabeshima, *Dev. Biol.*, 2004, **269**, 447-458.

46. V. K. Saxena, R. Deb, S. Shrivastava, C. Kantaraja, A. Kumar and S. Kumar, *Res. Vet. Sci.*, 2012, **93**, 1531-1536.

47. Y. Wang, X. H. Liu, J. L. Zhang, D. Aili and B. Liedberg, *Chem. Sci.*, 2014, **5**, 2651-2656.

48. Y. Takatsuji, S. Ikeno and T. Haruyama, *Sensors*, 2012, **12**, 4952-4961.

49. M. Retout, H. Valkenier, E. Triffaux, T. Doneux, K. Bartik and G. Bruylants, *ACS Sensors*, 2016, **1**, 929-933.

50. Y. Wang, X. H. Liu, P. Chen, N. T. Tran, J. L. Zhang, W. S. Chia, S. Boujday and B. Liedberg, *Analyst*, 2016, **141**, 3233-3238.

51. S. Tadepalli, Z. F. Kuang, Q. S. Jiang, K. K. Liu, M. A. Fisher, J. J. Morrissey, E. D. Kharasch, J. M. Slocik, R. R. Naik and S. Singamaneni, *Sci. Rep.*, 2015, **5**, 16206.

52. C. Wang, D. Liu and Z. Wang, *Chem. Commun.*, 2012, **48**, 8392-8394.

53. R. Chandrawati and M. M. Stevens, *Chem. Commun.*, 2014, **50**, 5431-5434.

54. B. D. Chithrani and W. C. Chan, *Nano Lett.*, 2007, **7**, 1542-1550.

55. J. M. de la Fuente and C. C. Berry, *Bioconjug. Chem.*, 2005, **16**, 1176-1180.

56. R. Lévy, *ChemBioChem*, 2006, **7**, 1141-1145.

57. L. Wei, Q. Y. Yang and L. H. Xiao, *Nanoscale*, 2014, **6**, 10207-10215.

58. H. Yuan, J. A. Gomez, J. S. Chien, L. N. Zhang, C. M. Wilson, S. Q. Li, A. M. Fales, Y. Liu, G. A. Grant, M. Mirotsou, V. J. Dzau and V. D. Tuan, *J. Biophotonics*, 2016, **9**, 406-413.

59. L. Sun, D. Liu and Z. Wang, *Langmuir*, 2008, **24**, 10293-10297.

60. T. T. Yin, W. J. Xie, J. Sun, L. C. Yang and J. Liu, *ACS Appl. Mater. Interf.*, 2016, **8**, 19291-19302.

61. S. Khamehchian, M. Nikkhah, R. Madani and S. Hosseinkhani, *J. Biomed. Mater. Res. A*, 2016, **104**, 2693-2700.

62. R. Shukla, E. Hill, X. Shi, J. Kim, M. C. Muniz, K. Sun and J. R. Baker, *Soft Matter*, 2008, **4**, 2160-2163.

63. M. J. Kogan, I. Olmedo, L. Hosta, A. R. Guerrero, L. J. Cruz and F. Albericio, *Nanomedicine*, 2007, **2**, 287-306.

64. Z. J. Li and C. H. Cho, *J. Transl. Med.*, 2012, **10**, S1.

65. S. Dufort, L. Sancey, A. Hurbin, S. Foillard, D. Boturyn, P. Dumy and J.-L. Coll, *J. Drug Target.*, 2011, **19**, 582-588.

66. D. Arosio, L. Manzoni, E. M. Araldi and C. Scolastico, *Bioconjug. Chem.*, 2011, **22**, 664-672.

67. M. B. Dowling, L. Li, J. Park, G. Kumi, A. Nan, H. Ghandehari, J. T. Fourkas and P. DeShong, *Bioconjug. Chem.*, 2010, **21**, 1968-1977.

68. P. Ghosh, X. Yang, R. Arvizo, Z.-J. Zhu, S. S. Agasti, Z. Mo and V. M. Rotello, *J. Am. Chem. Soc.*, 2010, **132**, 2642-2645.

69. L. Maus, O. Dick, H. Bading, J. P. Spatz and R. Fiammengo, *ACS Nano*, 2010, **4**, 6617-6628.

70. J. Wang, Y. Yue, G. Chen and J. Xia, *Soft Matter*, 2011, **7**, 7217-7222.

71. H. Yang, S. Y. Fung and M. Liu, *Angew. Chem. Int. Ed.*, 2011, **50**, 9643-9646.

72. B. Harper, F. Sinche, R. H. Wu, M. Gowrishankar, G. Marquart, M. Mackiewicz and S. L. Harper, *Nanomaterials*, 2014, **4**, 355-371.

73. D. Bartczak, S. Nitti, T. M. Millar and A. G. Kanaras, *Nanoscale*, 2012, **4**, 4470-4472.

74. N. Chanda, V. Kattumuri, R. Shukla, A. Zambre, K. Katti, A. Upendran, R. R. Kulkarni, P. Kan, G. M. Fent and S. W. Casteel, *Proc. Natl. Acad. Sci. USA*, 2010, **107**, 8760-8765.

75. L. Hosta-Rigau, I. Olmedo, J. Arbiol, L. J. Cruz, M. J. Kogan and F. Albericio, *Bioconjug. Chem.*, 2010, **21**, 1070-1078.

76. F. Silva, A. Zambre, M. P. C. Campello, L. Gano, I. Santos, A. M. Ferraria, M. J. Ferreira, A. Singh, A. Upendran, A. Paulo and R. Kannan, *Bioconjug. Chem.*, 2016, **27**, 1153-1164.

77. S. Wilhelm, A. J. Tavares, Q. Dai, S. Ohta, J. Audet, H. F. Dvorak and W. C. W. Chan, *Nat. Rev. Mater.*, 2016, **1**, 16014.

78. A. Kumar, H. Ma, X. Zhang, K. Huang, S. Jin, J. Liu, T. Wei, W. Cao, G. Zou and X.-J. Liang, *Biomaterials*, 2012, **33**, 1180-1189.

79. M. I. Gibson and R. K. O'Reilly, *Chem. Soc. Rev.*, 2013, **42**, 7204-7213.

80. A. Kumar, S. Huo, X. Zhang, J. Liu, A. Tan, S. Li, S. Jin, X. Xue, Y. Zhao and T. Ji, *ACS Nano*, 2014.

81. X. Ma, X. Wang, M. Zhou and H. Fei, *Adv. Healthc. Mater.*, 2013, **2**, 1638-1643.

82. W.-H. Chen, J.-X. Chen, H. Cheng, C.-S. Chen, J. Yang, X.-D. Xu, Y. Wang, R.-X. Zhuo and X.-Z. Zhang, *Chem. Commun.*, 2013, **49**, 6403-6405.

83. M. Akrami, S. Balalaie, S. Hosseinkhani, M. Alipour, F. Salehi, A. Bahador and I. Haririan, *Sci. Rep.*, 2016, **6**, 31030.

84. Y. L. Liu and S. Franzen, *Bioconjug. Chem.*, 2008, **19**, 1009-1016.

85. Y. Yi, H. J. Kim, P. Mi, M. Zheng, H. Takemoto, K. Toh, B. S. Kim, K. Hayashi, M. Naito, Y. Matsumoto, K. Miyata and K. Kataoka, *J. Controlled Release*, 2016, **244**, 247-256.

86. X. H. Yan, J. Blacklock, J. B. Li and H. Mohwald, *ACS Nano*, 2012, **6**, 111-117.

87. M. E. Muroski, T. J. Morgan, C. W. Levenson and G. F. Strouse, *J. Am. Chem. Soc.*, 2014, **136**, 14763-14771.

88. L. H. Peng, Y. F. Huang, C. Z. Zhang, J. Niu, Y. Chen, Y. Chu, Z. H. Jiang, J. Q. Gao and Z. W. Mao, *Biomaterials*, 2016, **103**, 137-149.

89. A. N. Shirazi, K. L. Paquin, N. G. Howlett, D. Mandal and K. Parang, *Molecules*, 2014, **19**, 13319-13331.

90. S. Patel, D. Jung, P. T. Yin, P. Carlton, M. Yamamoto, T. Bando, H. Sugiyama and K. B. Lee, *ACS Nano*, 2014, **8**, 8959-8967.

91. P. M. Tiwari, E. Eroglu, S. S. Bawage, K. Vig, M. E. Miller, S. Pillai, V. A. Dennis and S. R. Singh, *Biomaterials*, 2014, **35**, 9484-9494.

92. T. Morais, M. E. Soares, J. A. Duarte, L. Soares, S. Maia, P. Gomes, E. Pereira, S. Fraga, H. Carmo and M. D. L. Bastos, *Eur. J. Pharm. Biopharm.*, 2012, **80**, 185-193.

93. K. Cheng, S. R. Kothapalli, H. G. Liu, A. L. Koh, J. V. Jokerst, H. Jiang, M. Yang, J. B. Li, J. Levi, J. C. Wu, S. S. Gambhir and Z. Cheng, *J. Am. Chem. Soc.*, 2014, **136**, 3560-3571.

94. Z. M. Li, P. Huang, X. J. Zhang, J. Lin, S. Yang, B. Liu, F. Gao, P. Xi, Q. S. Ren and D. X. Cui, *Mol. Pharm.*, 2010, **7**, 94-104.

95. C. Roma-Rodrigues, A. Heuer-Jungemann, A. R. Fernandes, A. G. Kanaras and P. V. Baptista, *Int. J. Nanomed.*, 2016, **11**, 2633-2639.

96. N. Thovhogi, N. Sibuyi, M. Meyer, M. Onani and A. Madiehe, *J. Nanopart. Res.*, 2015, **17**.

97. Y. S. Chen, Y. C. Hung, I. Liau and G. S. Huang, *Nanoscale Res. Lett.*, 2009, **4**, 858-864.